

Superhydrophobic Chips for Cell Spheroids High-Throughput Generation and Drug Screening

Mariana B. Oliveira,^{†,‡} Ana I. Neto,^{†,‡} Clara R. Correia,^{†,‡} Maria Isabel Rial-Hermida,[§] Carmen Alvarez-Lorenzo,[§] and João F. Mano^{*,†,‡}

[†]3B's Research Group—Biomaterials, Biodegradables and Biomimetics, University of Minho, Headquarters of the European Institute of Excellence on Tissue Engineering and Regenerative Medicine, AvePark, 4806-909 Taipas, Guimarães, Portugal

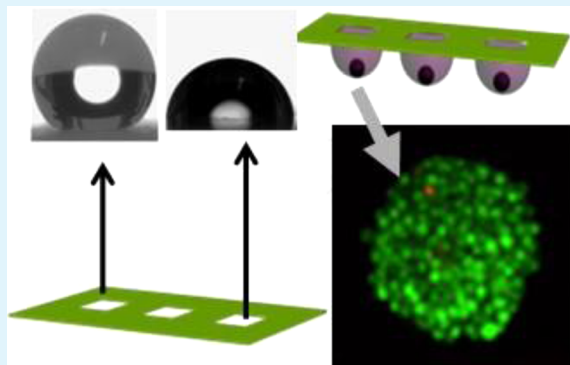
[‡]ICVS/3B's - PT Government Associate Laboratory, Braga/Guimarães, Portugal

[§]Departamento de Farmacia y Tecnología Farmacéutica, Universidad de Santiago de Compostela, 15782-Santiago de Compostela, Spain

W Web-Enhanced Feature S Supporting Information

ABSTRACT: We suggest the use of biomimetic superhydrophobic patterned chips produced by a benchtop methodology as low-cost and waste-free platforms for the production of arrays of cell spheroids/microtissues by the hanging drop methodology. Cell spheroids have a wide range of applications in biotechnology fields. For drug screening, they allow studying 3D models in structures resembling real living tissues/tumors. In tissue engineering, they are suggested as building blocks of bottom-up fabricated tissues. We used the wettability contrast of the chips to fix cell suspension droplets in the wettable regions and evaluated on-chip drug screening in 3D environment. Cell suspensions were patterned in the wettable spots by three distinct methods: (1) by pipetting the cell suspension directly in each individual spot, (2) by the continuous dragging of a cell suspension on the chip, and (3) by dipping the whole chip in a cell suspension. These methods allowed working with distinct throughputs and degrees of precision. The platforms were robust, and we were able to have static or dynamic environments in each droplet. The access to cell culture media for exchange or addition/removal of components was versatile and opened the possibility of using each spot of the chip as a mini-bioreactor. The platforms' design allowed for samples visualization and high-content image-based analysis on-chip. The combinatorial analysis capability of this technology was validated by following the effect of doxorubicin at different concentrations on spheroids formed using L929 and SaOs-2 cells.

KEYWORDS: superhydrophobic surfaces, high-throughput analysis, arrays, drug discovery, microtissues



INTRODUCTION

High-throughput studies in biotechnology areas such as drug screening and tissue engineering have been carried out mainly in two-dimensional (2D) environment. Such models are routinely used for evaluating the effectiveness and safety of libraries of drugs and other bioactive or potentially therapeutic molecules. However, biological phenomena in living organisms clearly take place in three-dimensional (3D) environments. In 2D techniques, cell-to-plastic interactions prevail rather than the crucial cell-to-cell and cell-to-extracellular matrix (ECM) interactions that form the basis for normal cell function. Tissue culture polystyrene is an unnaturally stiff substrate compared to the softer mechanical environment that cells experience in vivo. The stiffness of the substrates used for cell growth is well-known to alter cell function. For example, mesenchymal stem cells differentiation can be directed into certain lineages simply by altering the stiffness of the substrates they were cultured on.¹ In nature cells lie in a 3D configuration organized in the self-

secreted microenvironment, the ECM, both in organs and tumor masses. In this milieu, cells interact in a totally natural manner, without the intervention of foreign factors, such as biomaterials. The demand for studies using organotypic models is increasing, in order to improve the relevance of the findings achieved in these areas of study.

The use of cell spheroids has been suggested as a potential link to bridge the gap between monolayer cultures and animal model studies.^{2–6} A solution to create organotypic models is the in vitro construction of cell spheroids. Multicellular tumor spheroids were described as 'spherically symmetric aggregates of cells analogous to tissues, with no artificial substrate for cell attachment. Such cell structures resemble tumors in vivo in many ways. It is known that the expression of antigens, pH and

Received: March 27, 2014

Accepted: May 27, 2014

Published: May 27, 2014

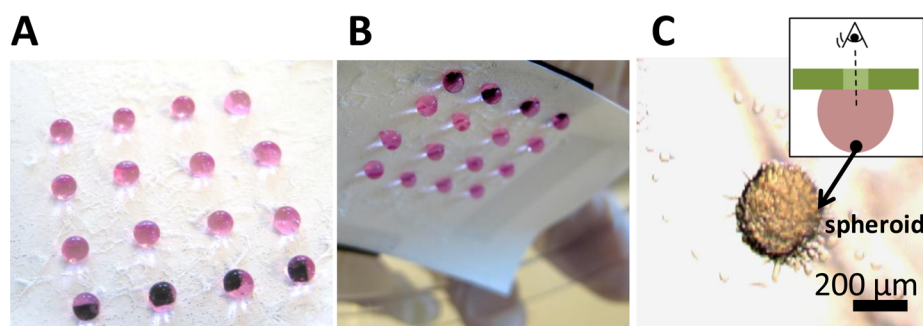


Figure 1. Pictures of the chips with the cell suspensions turned (A) upside and (B) tilted down. (C) Transmitted light microscopy image of a spheroid, observed from the top of the chip, through the transparent spot (as indicated in the schematic representation). Additional information on the robustness of the chips to movement can be found in Video 3.

oxygen gradients within the spheroid, as well as penetration rate of growth factors and distribution of proliferating/quiescent cells within the spheroid is similar to those of a real tumor.^{7,8} Resembling the *in vivo* environment, in those micromasses cells tend to attach each other in an organized structure constituted by cells in combination with ECM. Some types of spheroids are grown in order to mimic tumor models: the living spheroid structure contains a necrotic core, similarly to the native tumors.⁹ As such, the accessibility of cytotoxic agents into the spheroids may be limited by hypoxia and poor vascularization within the microregions of the cultures¹⁰ as occurs in solid tumors.^{11–13} Cell growth in 3D organization has been reported to induce significant variations in the bioenergetics of osteosarcoma cells (MG-63).¹⁴ In the cancer research field, cell spheroids have been widely applied as *in vitro* systems to investigate specific microenvironment factors associated with tumor therapy, such as the mechanism of action of chemotherapy, radiotherapy,^{15,16} and drug toxicity.¹⁷ Cell spheroids are also useful as models for the development of complex microtissues and can also be used as building blocks of larger tissues.^{18–20}

Several methods to produce cell spheroids can be found in literature.⁵ The hanging drop technique is an advantageous method since it can be applied to distinct cell types, it enables the control of the spheroid size control, and the micromass is exposed to low shear stress.²¹ The cells are pulled to the concave bottom of a hanging droplet by gravity effect, and tend to start the natural organization by cell–cell attachment and production of ECM. To make spheroids by the hanging drop technique, usually volumes of about 20–30 μL of a cell suspension are pipetted onto the inside lid of a tissue culture plate.²² Advances into high throughput production of spheroids using the hanging drop method have been made, producing up to 384 spheroids in a single array.²³ However, the platforms developed in that previous work were fabricated by injection molding, requiring specific processing machinery.

Herein, we suggest the use of superhydrophobic surfaces patterned with wettable regions as platforms produced by a benchtop methodology for the affordable and scale-up production and analysis of cell spheroids/microtissues by the hanging drop technique. Platforms based on wettability contrast were previously used for the high-content study of cells-biomaterials interactions.^{24–26} In such studies, the patterning of wettable regions in superhydrophobic polystyrene and poly(lactic acid) was performed by exposure to UV/ozone or plasma gas.^{27,28} In both cases, the wettability of the patterns was controlled by the time of exposure of the super-

hydrophobic surfaces to the UV/ozone or plasma treatments through a photomask. More recently, instead of patterning wettable regions in the polystyrene surfaces after the phase-separation treatment that leads to their superhydrophobicity, the authors suggested the protection of untreated commercial polystyrene with poly(vinyl chloride) (PVC) stickers, followed by the phase separation treatment of the polymeric surface.²⁹ The area protected by the stickers remained with the original contact angle of untreated polystyrene, as the surroundings were treated to be superhydrophobic. The patterning of wettable regions in other superhydrophobic polymeric surfaces was also reported for biotechnology applications. Accardo et al. reported the production of poly(methyl methacrylate) superhydrophobic surfaces by lithography and plasma etching for the X-ray scattering of protein solutions drying in surfaces with distinct topographies.³⁰ Such surfaces were more recently used for droplet mixing controlled by electrowetting, with great avoidance of contact between the droplets and the surface.³¹ We adapted polystyrene superhydrophobic platforms - with transparent wettable regions and the hanging drop surface totally exposed to the external media allowing its facilitated manipulation—as high-throughput screening platforms for drug testing and on-chip high-content cell response analysis by microscopy. In this approach, cell spheroids were produced by three methods, with distinct throughput abilities and adaptable to the needs of the user: (1) by manual pipetting of cell suspensions in each wettable regions, (2) by dragging a cell suspension on the chip and (3) by dipping the whole chip in a cell suspension.

For the proof-of-concept we dispensed cell suspensions of distinct cell types (L929 and SaOs-2) with different cell densities in the array of wettable regions of the chips. After the formation of cell spheroids, we tested the effect of a cytostatic agent used in clinical practice (doxorubicin - Dox), also dispensed in a combinatorial way in each individual spot of the chip. By on-chip microscopy analysis we proved the suitability of such platforms for direct drug screening using tumor-like models. The presence of transparent patterns in the chips allowed monitoring spheroids formation in real-time without the need of any staining, simply by using transmitted light microscopy. Moreover, the platforms were robust allowing for successive tilting, as the droplets do not slip from the wettable spot. We also proved that besides working directly in the wettable spots by pipetting, it was possible to perforate the superhydrophobic surfaces and feed/remove media from the spots by holes where needles were inserted. With this in mind, we also showed the compatibility of this easily prepared and

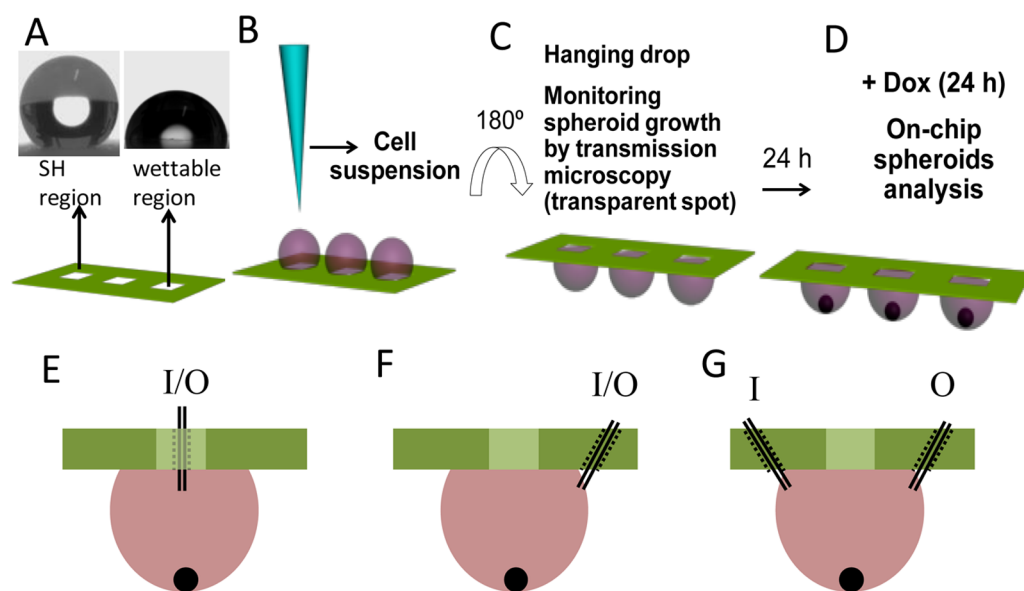


Figure 2. Schematic representation of the procedure for the production of spheroids in (A) superhydrophobic surfaces patterned with wettable transparent spots (water droplet profiles on the superhydrophobic region, left, and wettable region, right). (B) Addition of a cell suspension into the wettable spots of a superhydrophobic patterned chip by pipetting (method 1). (C) Turning of the platform 180° to create a hanging-drop setup. The spheroids were let to form for 24 h. (D) Dox was added to each well in combinatorial logic. The addition of Dox to the spots was performed by pipetting after tilting the chips (around 110°). However, the system was also adapted in order to avoid moving the platform, which may disturb the normal formation of the spheroids. We modified the system by making small holes (represented in dashed lines), to achieve multiple configurations with the same platform. (E) We perforated the inner part of the wettable regions of the array, in order to add and remove medium directly from the spot. (F) In another configuration, to avoid evaporation and contamination of the medium, we drilled the superhydrophobic region of the chip, 1 mm away from the wettable spot. As such, we accessed the medium laterally. (G) The number of holes in the system could be increased, and their position could be changed. For example, we created a two-entrance system, with an inlet (I) and an outlet (O), so the medium had a dynamic composition over time (Video 4, configuration F).

versatile system with dynamic media exchange and possible configurations that may allow in the future, for example, controlling the delivery of molecules over time, or to use each spot as a mini-bioreactor.

MATERIALS AND METHODS

Superhydrophobic Chips for Manual Pipetting Technique (Methodology 1). Polystyrene flakes were cut from commercially available polystyrene plates (Corning). PVC stickers (Oracal, U.S.A.) were glued in the polystyrene surface in the form of an array of $1 \times 1 \text{ mm}^2$ squares separated by 4 mm. Tetrahydrofuran (THF) was from Fluka (p.a.>99.5%) and ethanol absolute from Panreac. The surfaces were modified according to a phase separation protocol described elsewhere.³² The wettability of the surfaces was evaluated by contact angle (CA) measurements in an OCA15+ goniometer (DataPhysics, Germany) using the sessile drop method. The stickers were then removed from the surface of the chip. The protected regions remained untreated and, consequently, wettable and transparent (Figure 1A and B). Prior to the contact with cell suspension, the platforms were sterilized with ethanol 70% (v/v) for 2 h, rinsed with sterile phosphate buffered saline (PBS) 3 times and let to dry at room temperature.

Cell Expansion and Cell Culture. A fibroblast (L929) and an osteosarcoma cell line (SaOs-2) were used for spheroids formation and drug screening studies. Cells were expanded in basal medium consisting of DMEM (Gibco, UK) supplemented with 10% heat-inactivated fetal bovine serum (BiocromAG, Germany) and 1% antibiotic/antimycotic solution (penicillin 100 units/mL and streptomycin 100 mg/mL; Gibco, UK). Cells were grown in 150 cm^2 tissue culture flasks and incubated

at 37 °C in a humidified air atmosphere of 5% CO_2 . Every 3–4 days, fresh medium was added. At 90% of confluence, cells grown in tissue culture flasks were washed with PBS and subsequently detached by a chemical procedure with 0.05% trypsin-EDTA solution for 5 min at 37 °C in a humidified air atmosphere of 5% CO_2 . To inactivate the trypsin effect, cell culture medium was added. The cells were then centrifuged at 300 g and 25 °C for 5 min and the medium was decanted. Cell suspensions with distinct densities were prepared.

Spheroids Formation for Drug Screening. The chips were fixed to the lids of tissue culture plates using commercially available tape. The lower part of the plate was filled with sterile PBS, so the environment was saturated with water, to avoid the cell suspension droplets evaporation. A volume of $5 \mu\text{L}$ of cell suspensions of 4×10^6 and 8×10^6 cells/mL was dispensed in each wettable spot of the chip, as indicated in Figure 2. Each condition was processed in triplicate in each chip. The spheroids were let to form during 24 h, after turning the platforms 180°, by closing the tissue culture plate with the lid where the platform was fixed with tape. We were able to monitor the spheroids by transmitted light microscopy (Axio Imager Z1m, Zeiss), as the visible light was able to pass through the polystyrene transparent window in the chip.

Drug Screening: Studies with Doxorubicin. After 24 h of cell culture for spheroid formation, a volume of $1 \mu\text{L}$ of solutions of doxorubicin in water was added to each spot in the concentrations of 0, 0.1, 1, 10 μM (based on concentrations previously used).³³ As live/dead microscopy images from fluorescence microscopy showed a high resistance from L929 cells to these drug concentrations (Figure S1, Supporting Information), a new experiment was carried out with these cells

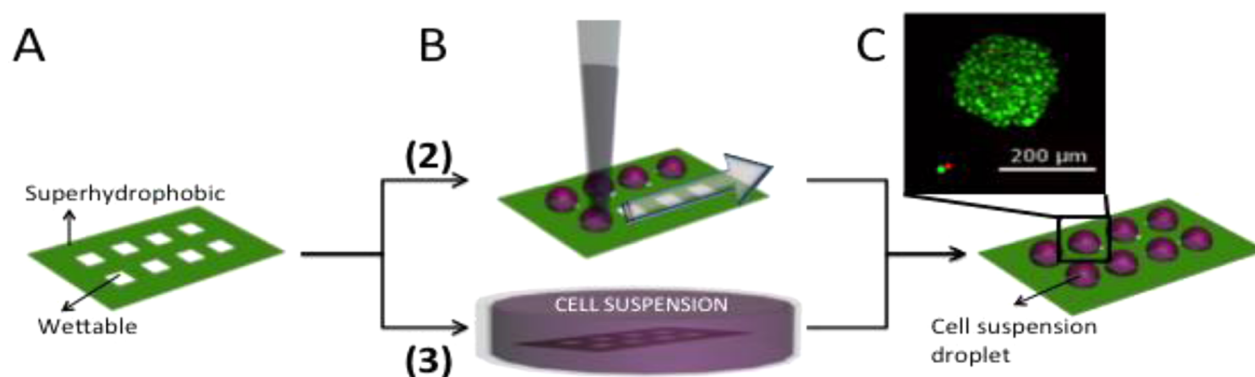


Figure 3. Schematic representation of the higher throughput methodologies (described as methods 2 and 3 in the text). (A) In both methodologies the superhydrophobic chip based on wettability contrast is used. (B) In methodology 2, presented in Video 1, a cell suspension is dragged through chip, and the droplets are fixed in the wettable spots because of the wettability contrast. In methodology 3, presented in Video 2, the whole chip is immersed in a cell suspension. When the chip is removed from the cell suspension, droplets are fixed in the wettable regions and the remaining liquid is repelled from the superhydrophobic parts of the surface due to its self-cleaning properties. (C) A chip with droplets of cell culture medium is obtained and then turned 180° for the formation of cell spheroids, in the same way as in methodology 1. Live/dead staining image of a cell spheroid obtained using the methodology 3.

with 0, 1, 10, and 100 $\mu\text{g}/\text{mL}$ of Dox (based on concentrations previously used).³⁴

Fluorescence Microscopy and Confocal Microscopy.

For fluorescence reflected light microscopy as well as for confocal microscopy, live dead staining was carried out using calcein AM and propidium iodide. A volume of 2 μL of solution of PBS with 10% (v/v) of each reagent was added to the spheroids, after 3 μL of the culture medium (from a total volume of 5 μL) was removed from the spots. The samples were left to incubate at 37 °C during 30 min, and then washed 3 times with 3 μL of PBS. Spheroids diameter quantification was carried out using ImageJ software (NIH, USA).

Viability Study: Image Quantification. Confocal microscopy images were used to determine cell viability. As such, we could determine the number of viable cells in each stack, even if the distribution of dead cells was not uniform in the spheroid. We used the particle analysis application of ImageJ software and analyzed the multiimages (multitiff) in the form of images stacks. The total number of cells in the analyzed spheroids was assumed to be the sum of cells counted in all stacks. Cell viability was determined as

$$\text{cell viability (\%)} = \frac{\sum \text{live cells}}{\sum (\text{live cells} + \text{dead cells})} \times 100\% \quad (1)$$

Superhydrophobic Chips for Higher-Throughput Techniques and Respective Spheroids Formation.

We treated the polystyrene chips with the PVC stickers, prepared as previously described for manual pipetting, with a layer of WX2100 (Cytonix, USA), an air-cured fluoro-urethane alkyd, according to the manufacturer's indications. This product has been previously used for cell studies without any report of cytotoxic effect.³⁵ For these studies, we used chips with stickers with 3 \times 3 mm², separated by 3 mm. The surfaces were then left dry for 48 h. We then removed the stickers.

For the method 2, as indicated in Figure 3A and B, we used a L929 cell line cell suspension with a density of 1 \times 10⁷ cells/mL. We dragged the cell suspension with a speed of approximately 1 wettable spot/second, as can be seen in Video 1. To measure the average volume of cell suspension fixed in each wettable spot, we used a micropipet and removed the medium from each individual spot. The chips were turned

180°, as for method 1, and the spheroids were let to form during 24 and 72 h. Live dead staining was carried out using calcein AM and propidium iodide, as described for method 1. The spheroids were then observed using reflected light fluorescence microscopy (Axio Imager Z1m, Zeiss), and their diameter was quantified using ImageJ software (NIH, USA).

For method 3, as indicated in Figure 3A and B, we used a L929 cell suspension with a density of 5 \times 10⁶ cells/mL. We dipped the whole chip in cell suspension during 5 s (as shown in Video 2). After removing the chip, we tilted it so the remaining cell suspension was removed from the superhydrophobic part of the chip. To measure the average volume of cell suspension fixed in each wettable spot, we used a micropipet and removed the medium from each individual spot. The chips were turned 180°, as in method 1, and the spheroids were left to form during 24 h. Live dead staining was carried out in the same conditions as for method 1. The spheroids were then observed using reflected light fluorescence microscopy (Axio Imager Z1m, Zeiss), and their diameter was quantified using ImageJ software (NIH, USA).

Increasing the Versatility of the Superhydrophobic Patterned Chips: Improving the Access to Cell Culture Medium.

Polystyrene surfaces prepared for drug screening studies (method 1) were perforated both in the center of the transparent spot (configuration D, Figure 2) or at 1 mm from the border of the transparent squares (configurations E and F, Figure 2), using a 27G needle for perforation. The needle tips were cut to be straight. They were introduced in the chip spot from the upper surface of the chip, as indicated in Figure 2, for medium exchange and circulation. We performed and tested the three configurations shown in Figure 2E–G. The liquid flows were adjusted to 60 $\mu\text{L}/\text{min}$ using a peristaltic pump.

Statistical Analysis. All cell spheroids diameter and cell viability quantification results were analyzed by one-way ANOVA with Tukey's post-test using GraphPad Prism software.

RESULTS AND DISCUSSION

By using the wettability contrast of the superhydrophobic patterned chip, we dispensed droplets of cell suspensions and kept them restricted and fixed in the wettable spot due to the difference in surface tension compared with the super-

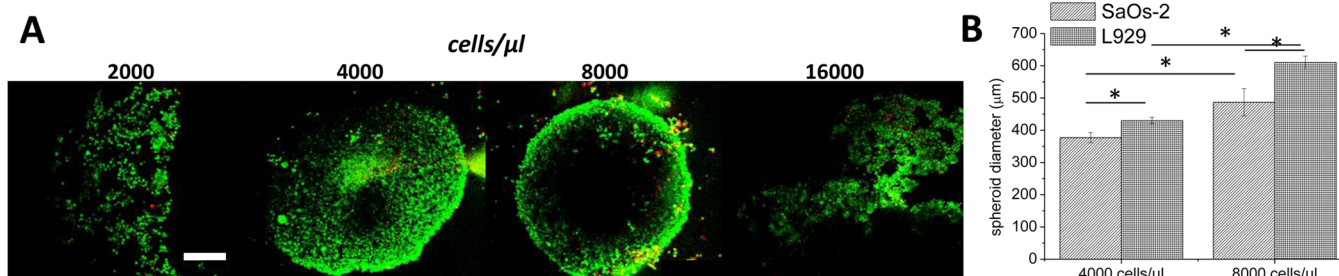


Figure 4. (A) Confocal assembly microscopy images of the cells after 24 h in the hanging drop system, dispensed in the wettable spots by manual pipetting. We observed that the conditions 4×10^6 and 8×10^6 cells/mL were the most favorable for spheroid formation. Scale bar = 200 μm . (B) Average diameter of the spheroids after 48 h of cell culture, without the addition of any drug. The asterisk (*) indicates significant differences for $p < 0.05$.

hydrophobic surrounding regions (Figure 1A). It was previously shown that protein adsorption in the wettable regions of the chips is higher than in the superhydrophobic parts.^{27,36} Moreover, cell adhesion and proliferation were, as well, diminished in the superhydrophobic parts of chips constituted by different polymers. Such results were observed for fibroblast and osteoblast-like cell lines in polystyrene, bone marrow stem cells in poly(lactic acid), NIH 3T3 fibroblasts in poly(methyl methacrylate), polyether ether ketone and poly-1,8-octanediol-*co*-citric acid surfaces, as well as for HEK 293 cells in poly(butyl methacrylate-*co*-ethylene dimethacrylate) surfaces.^{26,27,37–39}

Patterning of Cell Suspensions in the Chips. Cell suspensions were patterned in the wettable spots by manual pipetting of the cell suspension in each individual wettable pattern (Figure 2, describing method 1), dragging of a cell suspension in the array (Figure 3A and B, method 2), or dipping of the whole platform in the cell suspension (Figure 3A and B, method 3). The working principle behind all strategies is the wettability contrast in the chips, where the cell suspensions remain attached to the wettable spots and are repelled from the superhydrophobic regions because of its self-cleaning properties. However, their diversity allows choosing a higher-throughput and time-saving method for microtissue preparation, in the case of methods 2 and 3, or higher degree of control of the composition of each individual spot, in the case of method 1. The methods may also be combined. For example, cell spheroids may be prepared by method 2, if distinct types of spheroids are needed in replicate in the chips, or by method 3, if we aim to produce or study a single type of cell spheroid. Afterward, distinct drug formulations or other components may be dispensed in each individual spot by pipetting (method 1).

We observed that the chip could be rotated and tilted several times without any movement of the droplets (Figure 1B and Video 3). This proved that the handling of the chip, medium exchange and drug delivery to the droplet could be carried out easily, by simply tilting the culture plate lid, as shown in method 1. The superhydrophilic–superhydrophobic interactions in polystyrene superhydrophobic surfaces patterned with superhydrophilic channels were previously shown to be stable and resistant even to dynamic environment inside the channels. On the other hand, hydrophobic–superhydrophilic interactions in polystyrene did not allow restricting the liquid in the wettable patterns.³²

For method 2, using a micropipet to drag the cell suspension at an approximated rate of 1 wettable spot/second (Video 1), we observed that the volume fixed in each spot ranged from 6 to 7 μL . Cell spheroids were obtained from a cell suspension of

L929 (cell line generated from mice muscle fibroblasts), with a density of 1×10^7 cells/mL. After 24 h of cell culture, we obtained spheroids with mean sizes of $520.0 \pm 48 \mu\text{m}$ ($n = 20$), and after 72 h of cell culture with $800.3 \pm 18 \mu\text{m}$ ($n = 20$). As observed by the standard deviation of the spheroids size, a low size distribution was obtained using this approach. For method 3, we used chips with the same dimensions and immersed them for 5 s (Video 2). We observed that after dipping the volume of medium in each individual spot was also in the range of 6–7 μL . The cell suspension was in a concentration of 5×10^6 cells/mL. After 24 h of cell culture, we obtained spheroids with an average size of $205.6 \pm 26 \mu\text{m}$ ($n = 20$). With this method, the number of spheroids obtained in 5 s is solely dependent on the number of wettable regions on the chip.

As the wettable spots of the chips were transparent, the formation of spheroids was amenable to be monitored using transmitted light microscopy (Figure 1C), avoiding any cell staining or labeling using toxic labels. It also prevented excessive manipulation/opening of the lid, consequently decreasing the risk of contamination of the whole setup (Figure 2).

On-Chip Cell–Drug Interactions Tests. For the proof of concept of drug screening assays, L929 cells were first dispensed at distinct densities in the wettable spots (Figure 4A). After 24 h of incubation, we concluded that the densities that allowed forming cell spheroids were 4×10^6 and 8×10^6 cells/mL (Figure 4A). Using these conditions we produced spheroids of two cell types: L929 and SaOs-2 (cell line generated from a human osteosarcoma). Spheroids diameter was dependent on both cell number and cell type. For both cell types, after 48 h of incubation 8×10^6 cells/mL suspensions led to the formation of larger spheroids. Moreover, SaOs-2 spheroids were smaller than the ones constituted by L929 cells (Figure 4B).

The cell culture media was maintained static during spheroid formation time (24 h). Afterward, a cytostatic agent commonly used in clinical practice, Dox, was added in increasing doses. The influence of cell type and cell density of the suspension used to form the spheroid and drug concentration on cells viability was evaluated. Fluorescence microscopy pictures of live/dead staining of the spheroids are shown in Figure S1 (Supporting Information). Confocal microscopy stack images were used for an accurate cell number-based quantification; images resulting from the assembly of the stacks can be seen in Figure 5. For the first used Dox concentrations (0.1, 1, and 10 μM), SaOs-2 cells showed concentration-dependent cell viability. With increasing Dox concentration, the area corresponding to red cells (stained with propidium iodide)

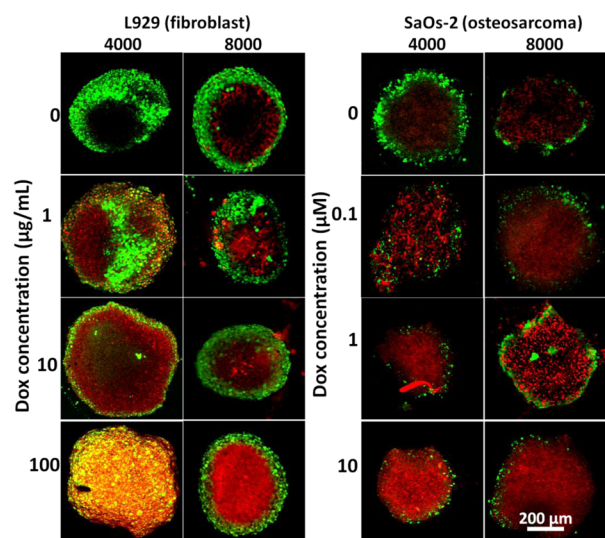


Figure 5. Confocal microscopy assembled images of the cell spheroids formed by L929 and SaOs-2 cells, with live (green)/dead (red) staining (calcein AM/propidium iodide).

increased (Figure S1, Supporting Information). However, we observed that for such concentrations the viability of L929 was maintained up to 48 h (Figure S1, Supporting Information). A decrease in L929 viability was only observed after 72 h of exposure to Dox. It was previously described that Dox does not kill L929 cells at concentrations that profoundly reduce clonogenic survival ($5 \mu\text{g/mL}$), corresponding to the range of concentrations used first in the work presented herein. Instead, the cell and nuclear volume progressively increase for at least 1 week following drug exposure leading to the production of characteristic giant cells. The increase in nuclear volume results from a continued DNA synthesis and increase in chromosome number without entry into mitosis.⁴⁰ As such, we performed the assays with higher concentrations, effective on L929 viability decrease, according to values reported elsewhere.²⁸ On the other hand, Dox was found to induce reactive oxygen species formation, mitochondrial membrane depolarization, mitochondrial cytochrome c release, caspase-3 activation, and apoptosis in SaOs-2 cells. As such, these cells are well-known as highly sensitive to Dox, even at low concentrations.⁴¹

We increased the amount of Dox added to L929 cell spheroids in the order of a million times, compared to the

originally used concentrations, and kept the values of the concentration used for SaOs-2. Then the percentage of living cells in the spheroids was quantified by analyzing the stacks of confocal microscopy images, with live/dead staining (Figure 5). Even with 10^6 -fold higher concentration of Dox (1, 10, and $100 \mu\text{g/mL}$), L929 cells were still significantly more resistant to this cytostatic than SaOs-2 cells. SaOs-2 cells viability showed a concentration-dependent behavior (Figure 6). For both cells types, 8×10^6 cells/mL spheroids showed lower viability than 4×10^6 cells/mL spheroids, even without the addition of Dox (Figure 6). This may be explained by the necrotic core formed in the 8×10^6 cells/mL spheroids after 24 h of cell culture (Figure 6), as they are much more compact than the 4×10^6 cells/mL spheroids: for a cell number twice as high, the diameter of the spheroids showed to be similar to the ones formed from the 4×10^6 cells/mL suspension. This fact probably limited oxygen and nutrients diffusion to the center of the cell mass.

Adaptation of the Chips for Dynamic Cell Environment. We adapted the chips to open the possibility of having dynamic cell environments where, for example, physiological-like drug delivery conditions and clearance properties could be mimicked. Three different possible configurations were tested. The first one (depicted in Figure 2E) consisted of holes in the middle part of the wettable regions of the chips, allowing exchanging medium in a direct manner by the introduction of a needle. However, such design may increase the evaporation of the medium from the spots and also increase contamination risk due to cell medium exposure to the outer environment. The second approach (shown in Figure 2F) consisted of a hole equivalent to the one of the configuration in Figure 2E, with the exception that the drilling was performed in the super-hydrophobic part of the chip, 1 mm away from the border of the wettable spots. Such configuration also allows expanding the number of inlets to the system, as shown in the third configuration (depicted in Figure 2G), where one of the holes is used as an inlet, and the second hole is used as an outlet. This configuration allows several approaches, such as recirculation of medium, physiological clearance mimetics, controlled drug delivery to the system, among others. We adjusted the flow of the inlets to $60 \mu\text{L/min}$ and were able to fill independently each well without having to turn the chip upsides. We additionally tested the system by filling and emptying the wettable spot with a red colorant (Video 4).

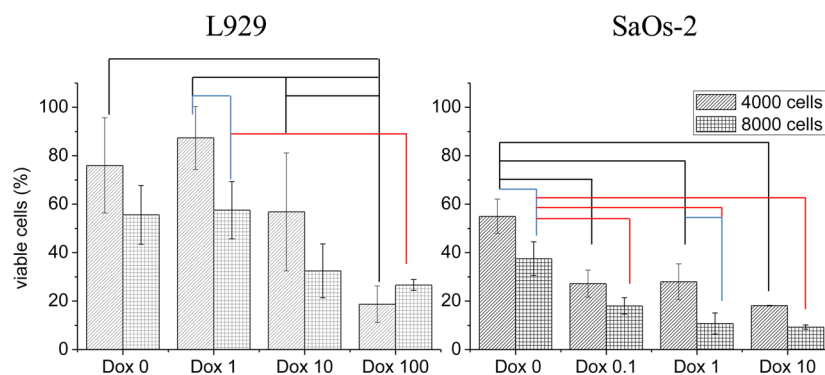


Figure 6. Quantification of viable cells by image analysis for L929 and SaOs-2 spheroids. The black lines indicate significant differences between distinct Dox concentrations for 4×10^6 cells/mL conditions, while red lines indicate significant differences between distinct Dox concentrations for 8×10^6 cells/mL conditions. Blue lines indicate significant differences between spheroids prepared using cell suspensions with distinct cell densities, but exposed to the same Dox concentration. Statistically differences were considered for $p < 0.05$.

Advantages of the Method and Future Perspectives.

In resume, superhydrophobic surfaces patterned with wettable regions are herein proposed as chips for the high-throughput generation and image acquisition of cell spheroids. We were able to pattern cell suspensions with precision in wettable spots by three distinct methods, with distinct throughputs. The superhydrophobic/wettable contrast in the chips allowed having stable droplets, whose volume was amenable to be varied by varying the size of the wettable spots. Because of the transparency of the wettable spots where cell suspensions were dropped, the platform is compatible with reflected light microscopy as well as transmitted light microscopy. The number of spheroids to be prepared was totally controlled by cutting the flexible polystyrene platform with a specific number of wettable regions, making the technique waste-free. The platform was totally two-dimensional, facilitating sterilization process and eventual reuse. After immersion in 70% ethanol (v/v) and drying at room temperature the chips remained superhydrophobic. Moreover, the borders of the wettable patterns designed in the chips remained defined, allowing reusing the platforms. We studied the effect of the addition of a cytostatic drug in different concentrations on the viability of two distinct cell types cultured in the form of spheroids. The platform is versatile as it allowed working with distinct types of cells, drug solutions and stainings. In future studies, it may be adapted for the study of complex heterotypical spheroids, composed by two or more cell types, in contact with distinct drugs, mixtures of drugs and agents released into the medium in a controlled fashion. We also proved that these chips are amenable to be adapted to bioreactor logic, where the flow of medium in each spot could be controlled independently. Clearance and renovation of solutions may be easily achieved by this method. The transparent window may also be useful in the future to monitor tissue formation and organization using cells transfected with fluorescent molecules. For example, the formation of Janus-like structures may be studied. Moreover, the ideal conditions that lead to the self-assembly of tissues mimicking their natural behavior in vivo, namely, their vascularization, may also be evaluated using these platforms.^{42,43}

CONCLUSIONS

Superhydrophobic surfaces patterned with wettable spots were successfully used as improved and versatile platforms for high-throughput spheroids formation and drug screening in such in vitro-constructed tissues. These affordable chips are easy to design and can be produced by a benchtop strategy. They are totally cytocompatible and allow working in contamination-preventing visualization conditions. We proved that they are robust and adequate for combinatorial high-throughput drug screening tests. Moreover, we were able to modify them as mini-bioreactors with several configurations that may be used to distinct applications needs, with distinct behaviors in each spot. We believe these platforms may find application in future works regarding not only drug screening but also microtissues formation for tissue engineering purposes.

ASSOCIATED CONTENT

Supporting Information

Figures regarding drug testing on-chip. This material is available free of charge via the Internet at <http://pubs.acs.org>.

Web-Enhanced Features

Videos showing the dynamic medium in each spot on the chip and higher-throughput methods to produce cell spheroids are available in the HTML version of the paper.

AUTHOR INFORMATION

Corresponding Author

*E-mail: jmano@dep.uminho.pt.

Notes

The authors declare no competing financial interest.

ACKNOWLEDGMENTS

The authors acknowledge Fundação para a Ciência e para a Tecnologia for the PhD grants SFRH/BD/71396/2010 (M.B. Oliveira), SFRH/BD/73119/2010 (A.I. Neto), and SFRH/BD/69529/2010 (C.R. Correia). The research leading to these results has received funding from the European Union's Seventh Framework Programme (FP7/2007-2013) under grant agreement REGPOT-CT2012-316331-POLARIS. The research was also funded by FEDER through the Competitive Factors Operation Program—COMPETE, Portugal National funds through FCT—Fundação para a Ciência e a Tecnologia (PTDC/CTM-BIO/1814/2012) and Spain MINECO (SAF 2011-22771 and PRI-AIBPT-2011-1211). We also acknowledge Nuno M. Oliveira for helping with video shooting.

REFERENCES

- (1) Engler, A. J.; Sen, S.; Sweeney, H. L.; Discher, D. E. Matrix Elasticity Directs Stem Cell Lineage Specification. *Cell* **2006**, *126*, 677–689.
- (2) Minchinton, A. I.; Tannock, I. F. Drug Penetration in Solid Tumours. *Nat. Rev. Cancer* **2006**, *6*, 583–592.
- (3) Pampaloni, F.; Reynaud, E. G.; Stelzer, E. H. K. The Third Dimension Bridges the Gap between Cell Culture and Live Tissue. *Nat. Rev. Mol. Cell Biol.* **2007**, *8*, 839–845.
- (4) Kunz-Schughart, L. A.; Freyer, J. P.; Hofstaedter, F.; Ebner, R. The Use of 3-D Cultures for High-throughput Screening: The Multicellular Spheroid Model. *J. Biomol. Screening* **2004**, *9*, 273–285.
- (5) Breslin, S.; O'Driscoll, L. Three-Dimensional Cell Culture: The Missing Link in Drug Discovery. *Drug Discovery Today* **2013**, *18*, 240–249.
- (6) Meli, L.; Jordan, E. T.; Clark, D. S.; Linhardt, R. J.; Dordick, J. S. Influence of a Three-Dimensional, Microarray Environment on Human Cell Culture in Drug Screening Systems. *Biomaterials* **2012**, *33*, 9087–9096.
- (7) Hirschhaeuser, F.; Menne, H.; Dittfeld, C.; West, J.; Mueller-Klieser, W.; Kunz-Schughart, L. A. Multicellular Tumor Spheroids: An Underestimated Tool is Catching Up Again. *J. Biotechnol.* **2010**, *148*, 3–15.
- (8) Kim, J. B. Three-Dimensional Tissue Culture Models in Cancer Biology. *Semin. Cancer Biol.* **2005**, *15*, 365–377.
- (9) Peck, Y.; Wang, D.-A. Three-Dimensionally Engineered Biomimetic Tissue Models for In Vitro Drug Evaluation: Delivery, Efficacy and Toxicity. *Expert Opin. Drug Delivery* **2013**, *10*, 369–383.
- (10) Jang, S. H.; Wientjes, M. G.; Lu, D.; Au, J. L. S. Drug Delivery and Transport to Solid Tumors. *Pharm. Res.* **2003**, *20*, 1337–1350.
- (11) Sutherland, R. M.; Durand, R. E. Growth and Cellular Characteristics of Multicell Spheroids. *Recent Results Cancer Res.* **1984**, *95*, 24–49.
- (12) Santini, M. T.; Rainaldi, G.; Indovina, P. L. Apoptosis, Cell Adhesion, and the Extracellular Matrix in the Three-Dimensional Growth of Multicellular Tumor Spheroids. *Crit. Rev. Oncol./Hematol.* **2000**, *36*, 75–87.
- (13) Elliott, N. T.; Yuan, F. A Review of Three-Dimensional In Vitro Tissue Models for Drug Discovery and Transport Studies. *J. Pharm. Sci.* **2011**, *100*, 59–74.

- (14) Santini, M. T.; Rainaldi, G.; Romano, R.; Ferrante, A.; Clemente, S.; Motta, A.; Indovina, P. L. MG-63 Human Osteosarcoma Cells Grown in Monolayer and as Three-dimensional Tumor Spheroids Present a Different Metabolic Profile: a H-1 NMR Study. *FEBS Lett.* **2004**, *557*, 148–154.
- (15) Dubessy, C.; Merlin, J. L.; Marchal, C.; Guillemin, F. Spheroids in Radiobiology and Photodynamic Therapy. *Crit. Rev. Oncol./Hematol.* **2000**, *36*, 179–192.
- (16) Santini, M. T.; Rainaldi, G.; Indovina, P. L. Multicellular Tumour Spheroids in Radiation Biology. *Int. J. Radiat. Biol.* **1999**, *75*, 787–799.
- (17) Durand, R. E.; Olive, P. L. Resistance of Tumor Cells to Chemo- and Radiotherapy Modulated by the Three-Dimensional Architecture of Solid Tumors and Spheroids. *Methods Cell Biol.* **2001**, *64*, 211–233.
- (18) Mironov, V.; Visconti, R. P.; Kasyanov, V.; Forgacs, G.; Drake, C. J.; Markwald, R. R. Organ Printing: Tissue Spheroids as Building Blocks. *Biomaterials* **2009**, *30*, 2164–2174.
- (19) Ulloa-Montoya, F.; Verfaillie, C. M.; Hu, W. S. Culture Systems for Pluripotent Stem Cells. *J. Biosci. Bioeng.* **2005**, *100*, 12–27.
- (20) Schon, B. S.; Schrobback, K.; van der Ven, M.; Stroebel, S.; Hooper, G. J.; Woodfield, T. B. F. Validation of a High-throughput Microtissue Fabrication Process for 3D Assembly of Tissue Engineered Cartilage Constructs. *Cell Tissue Res.* **2012**, *347*, 629–642.
- (21) Achilli, T.-M.; Meyer, J.; Morgan, J. R. Advances in the Formation, Use and Understanding of Multi-cellular Spheroids. *Expert Opin. Biol. Ther.* **2012**, *12*, 1347–1360.
- (22) Lin, R.-Z.; Lin, R.-Z.; Chang, H.-Y. Recent Advances in Three-Dimensional Multicellular Spheroid Culture for Biomedical Research. *Biotechnol. J.* **2008**, *3*, 1172–84.
- (23) Hsiao, A. Y.; Tung, Y.-C.; Qu, X.; Patel, L. R.; Pienta, K. J.; Takayama, S. 384 Hanging Drop Arrays Give Excellent Z-factors and Allow Versatile Formation of Co-culture Spheroids. *Biotechnol. Bioeng.* **2012**, *109*, 1293–304.
- (24) Salgado, C. L.; Oliveira, M. B.; Mano, J. F. Combinatorial Cell-3D Biomaterials Cytocompatibility Screening for Tissue Engineering Using Bioinspired Superhydrophobic Substrates. *Integr. Biol.* **2012**, *4*, 318–327.
- (25) Oliveira, M. B.; Salgado, C. L.; Song, W.; Mano, J. F. Combinatorial On-Chip Study of Miniaturized 3D Porous Scaffolds Using a Patterned Superhydrophobic Platform. *Small* **2013**, *9*, 768–778.
- (26) Tsougeni, K.; Bourkoula, A.; Petrou, P.; Tserepi, A.; Kakabakos, S. E.; Gogolides, E. Photolithography and Plasma Processing of Polymeric Lab on Chip for Wetting and Fouling Control and Cell Patterning. *Microelectron. Eng.* **2014**, *124*, 47–52.
- (27) Neto, A. I.; Custodio, C. A.; Song, W. L.; Mano, J. F. High-Throughput Evaluation of Interactions Between Biomaterials, Proteins and Cells Using Patterned Superhydrophobic Substrates. *Soft Matter* **2011**, *7*, 4147–4151.
- (28) Song, W. L.; Veiga, D. D.; Custodio, C. A.; Mano, J. F. Bioinspired Degradable Substrates with Extreme Wettability Properties. *Adv. Mater.* **2009**, *21*, 1830–1834.
- (29) Oliveira, M. B.; Ribeiro, M. P.; Miguel, S. P.; Neto, A. I.; Coutinho, P.; Correia, I. J.; Mano, J. F. In Vivo High-Content Evaluation of Three-Dimensional Scaffolds Biocompatibility. *Tissue Eng. C* **2014**, DOI: 10.1089/ten.tec.2013.0738.
- (30) Accardo, A.; Gentile, F.; Mecarini, F.; De Angelis, F.; Burghammer, M.; Di Fabrizio, E.; Riekel, C. In Situ X-ray Scattering Studies of Protein Solution Droplets Drying on Micro- and Nanopatterned Superhydrophobic PMMA Surfaces. *Langmuir* **2010**, *26*, 15057–15064.
- (31) Accardo, A.; Mecarini, F.; Leoncini, M.; Brandi, F.; Di Cola, E.; Burghammer, M.; Riekel, C.; Di Fabrizio, E. Fast, Active Droplet Interaction: Coalescence and Reactive Mixing Controlled by Electrowetting on a Superhydrophobic Surface. *Lab Chip* **2013**, *13*, 332–335.
- (32) Oliveira, N. M.; Neto, A. I.; Song, W. L.; Mano, J. F. Two-Dimensional Open Microfluidic Devices by Tuning the Wettability on Patterned Superhydrophobic Polymeric Surface. *Appl. Phys. Express* **2010**, *3*, No. 085295.
- (33) Tan, M. L.; Friedhuber, A. M.; Dunstan, D. E.; Choong, P. F. M.; Dass, C. R. The Performance of Doxorubicin Encapsulated in Chitosan-Dextran Sulphate Microparticles in an Osteosarcoma Model. *Biomaterials* **2010**, *31*, 541–551.
- (34) Amjadi, I.; Rabiee, M.; Hosseini, M. S.; Mozafari, M. Synthesis and Characterization of Doxorubicin-Loaded Poly(Lactide-co-glycolide) Nanoparticles as a Sustained-Release Anticancer Drug Delivery System. *Appl. Biochem. Biotechnol.* **2012**, *168*, 1434–1447.
- (35) Hancock, M. J.; He, J. K.; Mano, J. F.; Khademhosseini, A. Surface-Tension-Driven Gradient Generation in a Fluid Stripe for Bench-Top and Microwell Applications. *Small* **2011**, *7*, 892–901.
- (36) Tsougeni, K.; Petrou, P. S.; Papageorgiou, D. P.; Kakabakos, S. E.; Tserepi, A.; Gogolides, E. Controlled Protein Adsorption on Microfluidic Channels with Engineered Roughness and Wettability. *Sens. Actuators, B* **2012**, *161*, 216–222.
- (37) Alves, N. M.; Shi, J.; Oramas, E.; Santos, J. L.; Tomás, H.; Mano, J. F. Bioinspired Superhydrophobic Poly(L-lactic acid) Surfaces Control Bone Marrow Derived Cells Adhesion and Proliferation. *J. Biomed. Mater. Res., Part A* **2009**, *91A*, 480–488.
- (38) Oliveira, S. M.; Song, W. L.; Alves, N. M.; Mano, J. F. Chemical Modification of Bioinspired Superhydrophobic Polystyrene Surfaces to Control Cell Attachment/Proliferation. *Soft Matter* **2011**, *7*, 8932–8941.
- (39) Ueda, E.; Levkin, P. A. Micropatterning Hydrophobic Liquid on a Porous Polymer Surface for Long-Term Selective Cell-Repellency. *Adv. Healthcare Mater.* **2013**, *11*, 1425–1429.
- (40) Lanks, K. W.; Lehman, J. M. Synthesis by L929 Cells following Doxorubicin Exposure. *Cancer Res.* **1990**, *50*, 4776–78.
- (41) Graat, H. C. A.; Witlox, M. A.; Schagen, F. H. E.; Kaspers, G. J. L.; Helder, M. N.; Bras, J.; Schaap, G. R.; Gerritsen, W. R.; Wuisman, P.; van Beusechem, V. W. Different Susceptibility of Osteosarcoma Cell Lines and Primary Cells to Treatment with Oncolytic Adenovirus and Doxorubicin or Cisplatin. *Br. J. Cancer* **2006**, *94*, 1837–1844.
- (42) Grellier, M.; Bordenave, L.; Amedee, J. Cell-to-Cell Communication Between Osteogenic and Endothelial Lineages: Implications for Tissue Engineering. *Trends Biotechnol.* **2009**, *27*, 562–571.
- (43) Rivron, N. C.; Liu, J.; Rouwkema, J.; de Boer, J.; van Blitterswijk, C. A. Engineering Vascularised Tissues In Vitro. *Eur. Cells Mater.* **2008**, *15*, 27–40.